A&A 566, A130 (2014)
DOI: 10.1051/0004-6361/201423750

Astronomy & Astrophysics

Doppler imaging of exoplanets and brown dwarfs⋆

Ian J. M. Crossfield

Max-Planck Institut für Astronomie, Königstuhl 17, 69117 Heidelberg, Germany
e-mail: ianc@lpl.arizona.edu

Received 3 March 2014 / Accepted 1 May 2014

ABSTRACT

Doppler imaging produces 2D global maps of rotating objects using high-dispersion spectroscopy. When applied to brown dwarfs and extrasolar planets, this technique can constrain global atmospheric dynamics and/or magnetic effects on these objects in unprecedented detail. I present the first quantitative assessment of the prospects for Doppler imaging of substellar objects with current facilities and with future giant ground-based telescopes. Observations will have the greatest sensitivity in K band, but the H and L bands will also be useful for these purposes. To assess the number and availability of targets, I also present a compilation of all measurements of photometric variability, rotation period (P), and projected rotational velocity ($v \sin i$) for all known brown dwarfs. Several bright objects are already accessible to Doppler imaging with currently available instruments. With the development of giant ground-based telescopes, Doppler imaging will become feasible for many dozens of brown dwarfs and for the few brightest directly imaged extrasolar planets (such as β Pic b). The present set of measurements of P, $v \sin i$, and variability are incomplete for many objects, and the sample is strongly biased toward early-type objects ($<L5$). Thus, surveys to measure these quantities for later-type objects will be especially helpful in expanding the sample of candidates for global weather monitoring via Doppler imaging.

Key words. instrumentation: spectrographs – techniques: spectroscopic – catalogs – planets and satellites: atmospheres – brown dwarfs – stars: imaging

1. Introduction

The use of high-dispersion, near-infrared (NIR) spectrographs is quickly advancing the study of brown dwarfs and extrasolar planets. Work in recent years has revealed the atmospheric composition and thermal structure of numerous short-period exoplanets (e.g., Snellen et al. 2010; Crossfield et al. 2011; Brogi et al. 2012; Rodler et al. 2012), the projected rotational velocity of the young exoplanet β Pic b (Snellen et al. 2014), and has produced the first 2D global map of patchy clouds on a brown dwarf (Crossfield et al. 2014). With a rapidly growing number of instruments suited to this work (see Table 1), the stage is set for exciting new developments in the fields of planetary and brown dwarf science.

The Doppler imaging map of the nearby brown dwarf Luhman 16B demonstrates the first opportunity to study global atmospheric dynamics and circulation and two-dimensional surface brightness variations – i.e., weather patterns – on planets and brown dwarfs beyond the Solar system. Photometric variability has been observed on brown dwarfs for many years (Tinney & Tolley 1999), with variability seen across all ages and spectral types (Joergens et al. 2003; Buenzli et al. 2014). Disk-integrated measurements of variability provide many significant insights into our understanding of brown dwarf atmospheres both in young star-forming regions (Joergens et al. 2003; Cody & Hillenbrand 2010) and for older objects in the field (Artigau et al. 2009; Radigan et al. 2012; Buenzli et al. 2012; Apai et al. 2013; Heinze et al. 2013) and just as they do for hot Jupiters (e.g., Knutson et al. 2012). But degeneracies inevitably preclude any unique determination of the brightness and geographic distributions of surface features from disk-integrated photometry (Cowan & Agol 2008; Cowan et al. 2013; Apai et al. 2013).

Doppler imaging can break these degeneracies. With appropriate regularization, the method produces a unique two-dimensional surface map of the entire visible surface of a rotating body. The technique dates back at least to Deutsch (1958) and has been recast and reviewed multiple times in the succeeding years (Vogt 1987; Piskunov & Rice 1993; Rice 2002). In brief, the approach takes high S/N rotationally-broadened line profiles and inverts modulations of these lines (induced by heterogeneous regions of differing abundances and/or surface brightness) into a global map using matrix-based or iterative forward-modeling approaches.

Doppler imaging of brown dwarfs is an exciting new development because in many ways these objects provide a direct proxy for studying planetary atmospheres. Previous Doppler imaging studies were limited to cool stars whose variability was traced to persistent or slowly-evolving magnetic starspots (e.g., Collier Cameron 1995; Hatzes 1998; Jardine et al. 1999; Strassmeier 2009), and the high-amplitude variability seen in young brown dwarfs likely results from similar processes (Joergens et al. 2003). Cooler, field brown dwarfs have essentially neutral photospheres and so magnetic effects are likely less important. Instead, variability in these objects is thought to be dominated by effects such as variable cloud thickness (Burgasser et al. 2002; Heinze et al. 2013) and global circulation and convection (Freytag et al. 2011; Showman & Kaspi 2013; Zhang & Showman 2014) – the same processes that dominate the observable atmospheres of Jupiter and the other Solar system gas giants.

In this paper, I present the first quantitative analysis of the prospects for Doppler imaging of brown dwarfs and of directly

⋆ Full Table 2 is available at the CDS via anonymous ftp to cdsarc.u-strasbg.fr (130.79.128.5) or via http://cdsarc.u-strasbg.fr/viz-bin/qcat?J/A+A/566/A130

Table 1. Active, planned, and notional high-resolution IR spectrographs.

Instrument	Resolution	Wavelength coverage	Telescope	Status	References
CSHELL	40 000	1–5 μm, ~0.0025λ coverage	IRTF (3 m)	Operating	Greene et al. (1993)
Phoenix	70 000	1–5 μm, ~0.005λ coverage	KPNO (4 m)	Operating	Hinkle et al. (1998)
ARIES	50 000	1–2.5 μm simultaneous	MMT (6.5 m)	Operating	McCarthy et al. (1998)
CRIRES	90 000	1–5 μm, ~0.02λ coverage[a]	VLT (8 m)	Operating[a]	Kaeufl et al. (2004)
IRCS	20 000	1–5 μm, ~0.2 μm coverage	Subaru (8 m)	Operating	Tokunaga et al. (1998)
NIRSPEC	20 000	1–5 μm, ~0.1λ coverage	Keck (10 m)	Operating	McLean et al. (1998)
IGRINS	40 000	1.5–2.5 μm simultaneous	McDonald (2.7 m)	Commissioning	Yuk et al. (2010)
GIANO	50 000	1–2.5 μm simultaneous	TNG (3.6 m)	Commissioning	Oliva et al. (2012)
ISHELL	72 000	1–5 μm, ~0.1λ coverage	IRTF (3 m)	Under construction	Rayner et al. (2012)
CARMENES	82 000	0.6–1.7μm simultaneous	Calar Alto (3.5 m)	Under construction	Quirrenbach et al. (2012)
SPIRou	75 000	1–2.4μm simultaneous	CFHT (3.6 m)	Under construction	Thibault et al. (2012)
IRD	70 000	1–1.75 μm simultaneous	Subaru (8 m)	Under construction	Tamura et al. (2012)
HPF	50 000	0.95–1.35 μm simultaneous	HET (9 m)	Under construction	Mahadevan et al. (2012)
HiJak	60 000	0.8–2.5 μm simultaneous	DCT (4.3 m)	Notional	Muirhead et al. (in prep.)
iLocater	100 000	0.95–1.1 μm simultaneous	LBT (8 m)	Planned	Crepp et al. (2014)
METIS	100 000	2.9–5.5 μm simultaneous	E-ELT (39 m)	Planned	Brandl et al. (2010, 2012)
HIRES	100 000	0.4–2.5 μm simultaneous	E-ELT (39 m)	Notional	Maiolino et al. (2013)
NIRES-B	20 000	1–2.5 μm simultaneous	TMT (30 m)	Notional	TMT Project (2013)
NIRES-R	100 000	3–5 μm simultaneous	TMT (30 m)	Notional	TMT Project (2013)
GMTNIRS	≥60 000	1–5 μm simultaneous	GMT (25 m)	Notional	Jaffe et al. (2006); Lee et al. (2010)

Notes. [(a)] CRIRES is scheduled to be upgraded during 2014–2017 to provide ~0.2λ coverage.

imaged giant extrasolar planets. These analyses indicate that while a few brown dwarfs are amenable to mapping with existing facilities, Doppler imaging will be feasible for dozens or hundreds of objects – both planets and brown dwarfs – with planned giant ground-based telescopes such as GMT, TMT, or E-ELT (Johns 2008; Nelson & Sanders 2008; Gilmozzi & Spyromilio 2007).

I also present a compilation of the rotational periods, photometric variability, and/or projected rotational velocities reported for all brown dwarfs and exoplanets. All of these quantities must be known before applying Doppler imaging to a target, and so the included catalog represents a first step toward a target list for future Doppler imaging efforts. In addition, such a catalog is useful for studies of, e.g., angular momentum, cloud properties, and physical sizes of substellar objects.

Section 2 describes the new catalog of measurements of variable and rotating substellar objects. Section 3 presents scaling relations for estimating the sensitivity of Doppler imaging efforts and estimates limiting magnitudes for various combinations of spectral type and telescope aperture. Finally, Sect. 4 concludes with a summary and final thoughts.

2. A new catalog of variable and rotating substellar objects

2.1. Compiling the catalog

To begin evaluating targets for Doppler imaging with the instruments summarized in Table 1, I have compiled a new database that contains all brown dwarfs and exoplanets for which published measurements exist of photometric variability, rotation periods (P), and projected rotational velocities ($v \sin i$). Figure 1 plots measurements of P, $v \sin i$, and photometric variability against spectral type. The catalog data are presented in Table 2 and the full data set is available online in machine-readable format.

In total the catalog contains 347 objects: 58 with reported rotation periods, 109 exhibiting variability in optical or infrared photometric bands, and 271 with measured $v \sin i$. For 23 objects, all three quantities have been measured. The electronic catalog includes spectral types[1] and JHK_s magnitudes from 2MASS (Skrutskie et al. 2006). The full set of references for all entries are included in the catalog and cited in the Appendix.

When an object's $v \sin i$ was measured by multiple groups, I report the weighted mean value; upper limits are also included. For rotation periods, I do not include the uncertainty on P which is often difficult to quantify and only infrequently reported. Variability measurements in the literature are more inhomogeneous in quality than are either P or $v \sin i$. Despite some concern regarding variability detections of questionable significance, recent observations demonstrate that for some brown dwarfs the amplitude of variability can change considerably from one epoch to the next (e.g., Gillon et al. 2013). I therefore liberally include all significant reports of previous variability, but I do not include null detections.

Figure 1 demonstrates that the catalog is dominated by early-type objects. Most measurements have been made for objects with earlier spectral types ($\lesssim$L5) because these intrinsically brighter objects are easier to detect and study at high signal-to-noise (S/N). Aside from the recently-discovered and well-studied T0.5 Luhman 16B (Luhman 2013), the coolest object with measured P, $v \sin i$, and photometric variability has spectral type L4. Much work remains to be done, then, in completely characterizing the late-type sample.

2.2. Rotational velocities and periods

As one example of the utility of such a database, Fig. 2 shows the 23 brown dwarfs with measured P and $v \sin i$. For known P, the upper limit to $v \sin i$ is $2\pi R/P$. For a radius of $R_{\rm Jup}$, this limit is indicated by the solid line in Fig. 2. Measurements indicate nine objects with radii $>R_{\rm Jup}$: four objects in young star forming regions, and five field objects. In order of increasing P, these objects are: field objects LP 349-25B, DENIS 1058-1548, 2MASS

[1] From http://www.dwarfarchives.org and the literature.

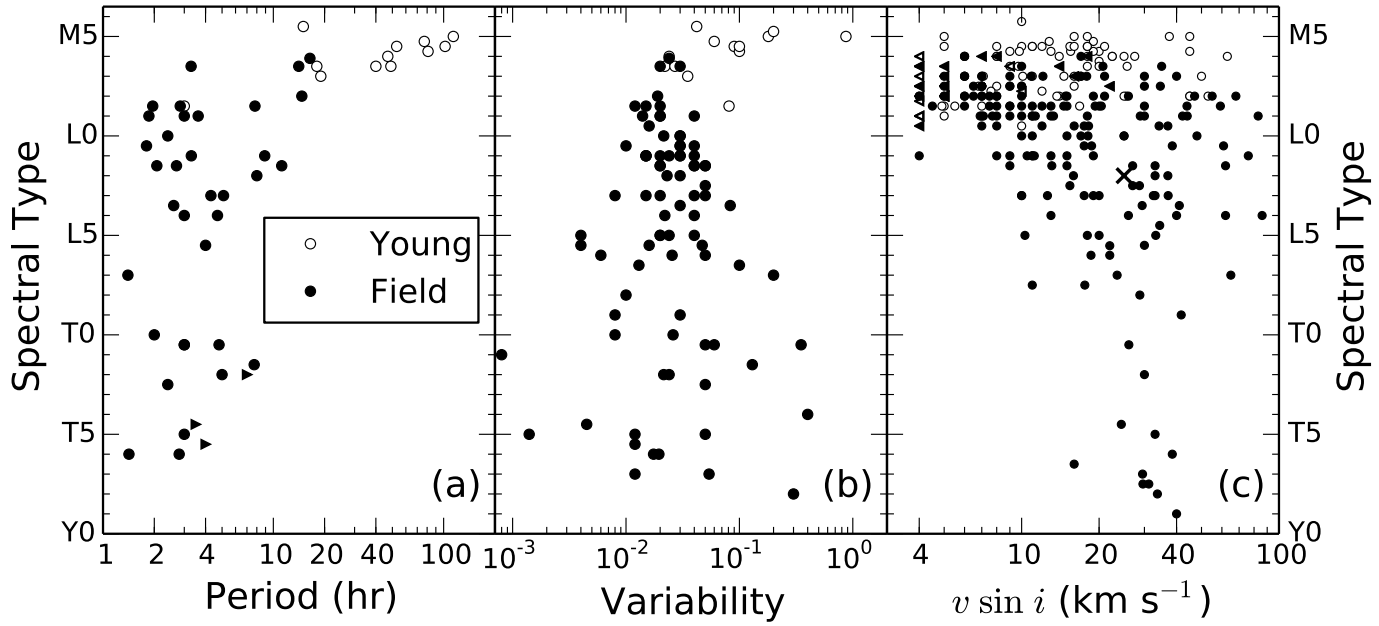

Fig. 1. Potential targets for future Doppler imaging: the full catalogue of measurements of substellar rotation and variability. The three panels show the spectral types of objects with measured rotation periods **a)**, photometric variability semi-amplitude in any bandpass **b)**, and $v \sin i$ **c)**. Upper limits to $v \sin i$, and lower limits on periods, are indicated by triangles. Solid points are field objects, empty points are young objects. The "×" symbol in panel **c)** indicates the young, giant exoplanet β Pic b (Snellen et al. 2014). See Table 2 for the full compilation and references. Note that the sample is quite incomplete for objects later than ~L5.

Table 2. Catalog of rotation and variability of substellar objects.

Object	RA (hh mm ss.s)	Dec (±dd mm ss.s)	$v \sin i$ (km s^{-1})	P (h)	ΔF (%)	Bandpass	Spectral type	Young? (Y/N)
GJ 1001B	00 04 34.8	–40 44 05.8	34.4 ± 1.8	–	–	–	L4.5	N
2MASS 0019262+461407	00 19 26.2	+46 14 07	68.0 ± 10.0	–	–	–	M8.0	N
2MASS 0019457+521317	00 19 45.7	+52 13 17	9.0 ± 2.0	–	–	–	M9.0	N
DENIS 0021-4244	00 21 05.9	–42 44 43.33	17.5 ± 2.0	–	–	–	M9.5	N
2MASS 0024246-015819	00 24 24.6	–01 58 20.14	34.2 ± 1.6	–	1.6	I	M9.5	N
2MASS 0024442-270825B	00 24 44.2	–27 08 25	9.0 ± 2.0	–	–	–	M8.5	N
LP 349-25A	00 27 55.9	+22 19 32.8	55.0 ± 2.0	–	–	–	M8	N
LP 349-25B	00 27 55.9	+22 19 32.8	83.0 ± 3.0	1.9	1.4	I	M9	N
...	...	...	...	...	...	...	...	...

Notes. The full table is available at the CDS in machine-readable form. A portion is shown here as an example of its content. References for all quantities are included in the machine-readable table, and for completeness are cited in the Appendix.

1146+2230AB, 2MASS 1146+2317, and LP 412-31; and young objects S Ori 25, and Cha Hα 3, 2, and 6.

Previous analyses of these objects are consistent with the conclusion that they must have radii $>R_{\rm Jup}$. Harding et al. (2013a) estimate the radius of LP 349-25B to be 1.45 $R_{\rm Jup}$, consistent with Fig. 2. Heinze et al. (2013) discuss the tension between various pieces of evidence in reconciling the rotational and physical parameters of DENIS 1058-1548, but favor a radius >1.1 $R_{\rm Jup}$. 2MASS 1146+2230AB is a close (0.3″) binary and it is not clear which component the literature values for P and $v \sin i$ refer to; nonetheless, the large $v \sin i$ = 32.5 km s^{-1} must be dominated by rotational effects. Bailer-Jones (2004) note that P and $v \sin i$ of both 2MASS 1146+2230AB and 2MASS 1146+2317 can be reconciled if $R \geq 1.3$ $R_{\rm Jup}$ and $\geq$0.95 $R_{\rm Jup}$, respectively, consistent with Fig. 2. Irwin et al. (2011) note that LP 412-31 must have $R > 1.1$ $R_{\rm Jup}$, consistent with Fig. 2. Measurements for the young substellar objects shown in Fig. 2 are also self-consistent because these objects are expected to be quite large (>7$R_{\rm Jup}$) on account of their young age (Joergens et al. 2003; Caballero et al. 2004).

In addition to these systems, 35 brown dwarfs have rotation periods but no reported $v \sin i$. High-resolution spectroscopy would more than double the current (P, $v \sin i$) sample, providing useful insights into brown dwarf evolution and (via gravity-sensitive features) help constrain absolute masses and radii of these objects.

3. Estimating sensitivity for Doppler imaging

Advances in Doppler imaging of substellar objects will rely primarily on improved instruments and telescopes. The first Doppler image of a brown dwarf was produced by observing an exceptional object – a 2 pc-distant T0.5 dwarf with K_s = 9.8 mag – with VLT/CRIRES, which offers high dispersion but a wavelength coverage of only 60 nm (Crossfield et al. 2014). Aside from a small number of brown dwarfs near the M/L transition, few other substellar objects are likely to be discovered that are so bright or so nearby. Yet Table 1 demonstrates that many spectrographs offering much broader wavelength coverage than CRIRES are currently under development.

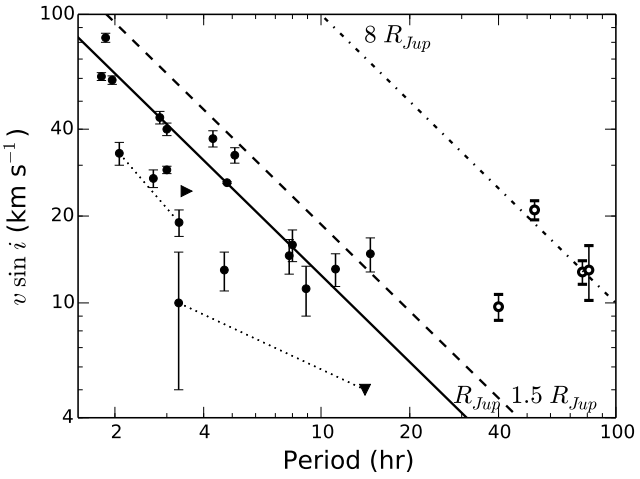

Fig. 2. Brown dwarfs with measured rotation periods and $v \sin i$. The curves show the maximum possible $v \sin i$ for the indicated radii. Open points are young substellar objects in the σ Ori or Cha I star forming regions. Dotted lines connect the components of binary systems. The triangles indicate upper or lower limits.

3.1. A rough sensitivity metric

As already discussed, successful Doppler imaging relies on precise measurements of the changing shapes of rotationally broadened absorption line profiles. One way to boost the precision is to increase the number of lines – and thus the total equivalent width (EW) – monitored in the analysis, either through techniques such as least-squares deconvolution (Donati et al. 1997) or through a full spectral synthesis approach. Precision will also increase when one obtains an intrinsically higher spectroscopic S/N – whether by observing a brighter target, using a larger telescope, or building a more efficient spectrograph. Finally, when all else is equal higher-fidelity maps can be made for objects exhibiting higher surface brightness heterogeneities; these are the features that manifest themselves as photometric variations with semi-amplitude ΔF.

Combining these factors produces a metric that describes how suitable a given target is for Doppler imaging. This "mapping sensitivity" metric is

$$M = \Delta F \times (S/N) \times \sum EW/2.5\ \mu\mathrm{m}. \quad (1)$$

The denominator is chosen to yield $M \approx 1.5$ for the initial Doppler imaging analysis of Luhman 16B, which provides a map that is useful but still rather noisy compared to analyses of brighter, stellar targets. I therefore suggest a cutoff of $M > 1$ as a rough rule of thumb. Objects falling below this threshold will yield only low-quality maps owing to being too faint, having too few strong absorption features, and/or having too nearly featureless a surface. The spectra of very late-type objects exhibit a nearly uninterrupted forest of often-weak absorption lines; a sufficiently high $v \sin i$ may blur these lines to such an extent that Doppler imaging is no longer feasible. The impact of this effect should be studied in the future, but the results below demonstrate that in the near term Doppler imaging will likely only be applied to objects with spectral types earlier than Luhman 16B.

Naturally, other factors will also influence the fidelity of a Doppler imaging analysis. For example, spectral resolution (R) limits the number of longitudinal (spatial) resolution elements around the resulting map to be roughly $n \leq Rv \sin i/c$ (Piskunov, priv. comm.). When observing over a single rotation period, the period P sets a similar limit of $n \leq P/t_{\rm int}$, where $t_{\rm int}$ is the effective integration time. Furthermore, the evolution of photometric variability varies considerably for different objects, ranging from short-term variations with little periodicity to strongly periodic signatures that repeat for many rotations: the latter objects in particular could be observed over many rotations to increase the quality of the desired Doppler image. In practice, a full simulation should be run for any target on the basis all known parameters: spectral morphology, brightness, rotation period, $v \sin i$, and amplitude and type of photometric variability. Nonetheless Eq. (1) is useful because it allows quick and simple evaluation of large numbers of targets.

3.2. Simulated observations

I next use the mapping sensitivity metric to estimate the feasibility of conducting Doppler imaging for various types of brown dwarfs using several representative observing facilities. This effort requires two components: a large set of brown dwarf spectra, and a simple model of a high-dispersion spectrograph.

Spectra were taken from the BT-Settl library, which provides high-resolution model surface fluxes for objects with effective temperatures from 400 K to 2600 K (Allard 2014). All models had surface gravities of 10^5 cm s^{-2} and used the abundance ratios of Caffau et al. (2011).

For the instrument, I developed a simple radiometric model of a high-dispersion NIR spectrograph. I use plausible values for the necessary instrument parameters, as compared to the various instruments listed in Table 1. The sky emission is appropriate for Mauna Kea and comes from the Gemini Observatory website[2]. I assume a slit width of 0.2″, a pixel scale of 0.1″ pixel^{-1} and $10^{-5}\ \lambda$ pixel^{-1}, a spectral resolution of 5×10^4, and a total instrumental throughput of 10%. Telluric transmission is taken from the high-resolution measurements of Hinkle et al. (2003). Each simulated spectrum is interpolated onto 2048 pixels spanning a wavelength range of 0.02λ, which approximates one echelle order and gives ~10 orders per telluric window. Finally, each simulated integration assumes 30 min of observing time: considering that brown dwarfs have rotation periods as short as 2 h (see Figs. 1 and 2), this integration time seems the longest likely to provide useful longitudinal resolution in a Doppler imaging analysis.

With this tool in hand, I compute the median S/N and the total EW of all absorption lines in each echelle order. The continuum level for computing EW values is determined by fitting a low-order polynomial to the brown dwarf's spectrum and iteratively rejecting points significantly below the fit. The S/N, total EW, and the mapping sensitivity (the product of S/N and EW) are plotted in Fig. 3 for three representative cases. To compute M I assume a photometric variability of $\Delta F = 3\%$, which is the median of the values in Table 2 and Fig. 1b.

To capture the benefits of the broad wavelength coverage offered by modern spectrographs, I compute sensitivity limits assuming a Doppler imaging analysis that uses a single photometric band. To the extent that many instruments listed in Table 1 can observe multiple bands simultaneously, this assumption underestimates the true sensitivity for a given target. The effective, broadband mapping sensitivity ($M_{\rm bb}$) is then the root-sum-square of all values of M computed as described above

[2] Currently at http://www.gemini.edu/sciops/telescopes-and-sites/observing-condition-constraints/ir-background-spectra; data there are based on the ATRAN model of Lord (1992).

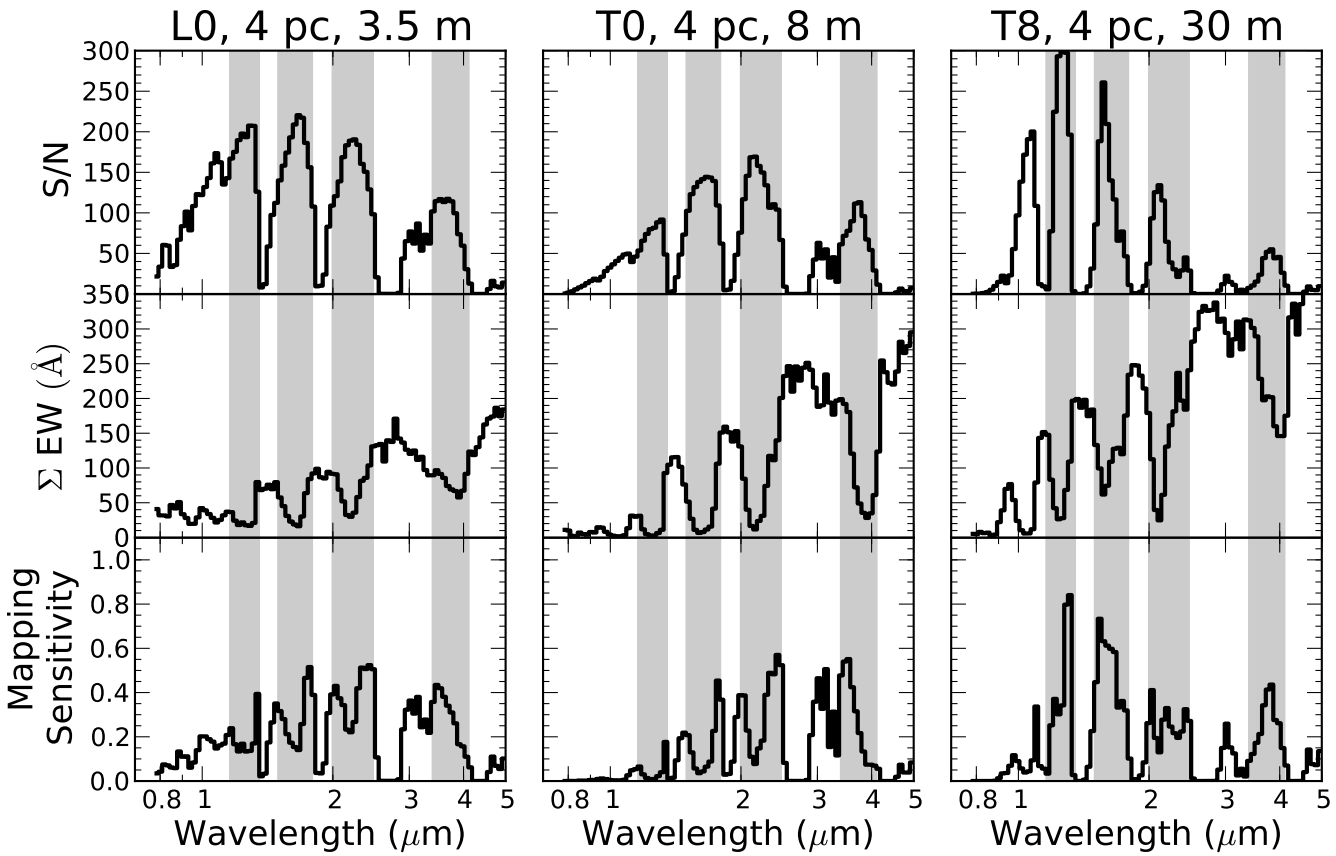

Fig. 3. Doppler imaging sensitivity analyses for three representative cases: an L0 dwarf observed with a 3.5 m telescope (*left*), a T0 with an 8 m telescope (*center*), and a T8 with a 30 m telescope (*right*), all located 4 pc away. From *bottom to top*, the plots show (in 0.02λ bins) the median S/N, total equivalent width of absorption lines, and the normalized product of these quantities. The root sum square of this last quantity over observable wavelengths determines the final Doppler imaging sensitivity of a given instrument. The gray regions indicate the wavelength regions used to calculate the magnitude limits shown in Fig. 4.

that lie within the specified bandpass. The limits I use are indicated by the gray regions in Fig. 3, and are: 1.16–1.35 μm, 1.5–1.79 μm, 2.0–2.47 μm, and 3.4–4.1 μm. From the definition of M in Eq. (1), a value of $M_{\rm bb} \geq 1$ for a given simulation indicates that Doppler imaging is feasible for the given combination of telescope, target effective temperature, and distance.

All these calculations provide an estimate of the greatest distance – or equivalently, the faintest apparent magnitude – an object could have and still be a useful target for Doppler imaging. These results are shown in Fig. 4 for three different telescope apertures (3.5 m, 8 m, and 30 m) for observations in each of the J, H, K, and L bandpasses. To make this plot, I converted the effective temperatures of the BT-Settl models to spectral type using the relation of Stephens et al. (2009).

In addition to the sensitivity limits, Fig. 4 shows the apparent magnitudes and spectral types of all substellar objects included in the catalog presented above. I approximate the L band magnitudes using the relation $K - L = 0.092T - 0.16$ (Fig. 1 of Golimowski et al. 2004), where T is the spectral type: 0 for M0, 10 for L0, etc. The scatter on this relationship is $\lesssim$0.2 mag, as estimated from the fits of spectral type vs. absolute magnitude relations for K band (Looper et al. 2008) and L band (Golimowski et al. 2004).

3.3. Results: feasibility of substellar Doppler imaging

Figure 4 indicates that K band is the optimal wavelength range for Doppler imaging of brown dwarfs. A high-dispersion spectrograph covering the K band could image an object like Luhman 16 – 2 pc distant, at the L/T transition – even on a <4 m telescope (see Fig. 4c). In contrast, the prospects at J band are the poorest of the wavelength ranges considered: Fig. 4a shows that Doppler imaging at these wavelengths will likely be feasible only with future giant ground-based telescopes. These results should not change so long as the amplitudes of brown dwarf variability does not hugely vary for these different bandpasses. For example, Fig. 4 shows that for a given brightness, an L/T transition dwarf would have to vary ~4× more at H band than at K band to provide comparable Doppler imaging sensitivity in both bandpasses. Multiwavelength observations demonstrate that the variability amplitudes of these objects are constant to within a factor of ~2 in different, broad bandpasses (Radigan et al. 2012; Buenzli et al. 2012; Biller et al. 2013).

In general, 3–4 m telescopes will be limited to the brightest objects at any given spectral type. Nonetheless Doppler imaging of several new brown dwarfs, especially the brightest targets near the M/L transition, should be feasible with these instruments. One example is the 4 pc-distant M9 dwarf 2MASS 1048147-395606, which has $v \sin i = 18 \pm 2$ km s^{-1} but no detections of photometric variability or rotation period.

Doppler imaging of more targets will become feasible with new, broad-wavelength-coverage spectrographs on 8 m telescopes. A few more later-type objects could be observed at K and/or L band. These include the T1 dwarf 2MASS J22431696-5932206 (for which 3% variability has been reported at I band, but P and $v \sin i$ have not been measured) and the rapidly-rotating

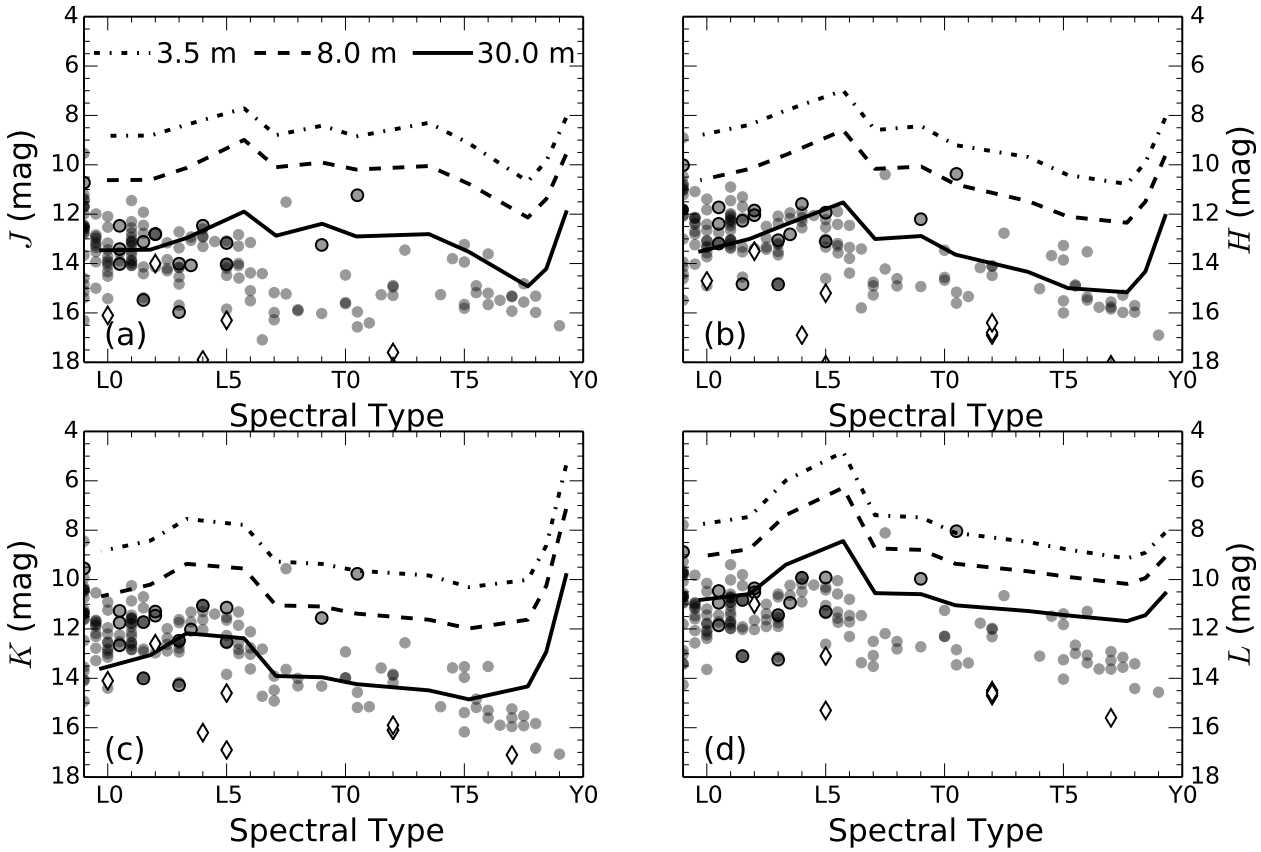

Fig. 4. Limiting infrared magnitudes for NIR Doppler imaging. Panels **a)–d)** show magnitude vs. spectral type for J, H, K, and L bands for a telescope either 3.5 m (dash-dotted), 8 m (dashed), or 30 m (solid) in diameter. Points indicate objects with measured rotational periods, photometric variability, and/or $v \sin i$. The best potential targets for Doppler imaging are indicated with black outlines, which have $v \sin i \geq 15$ km s^{-1} and/or vary photometrically by ≥2%. As described in Sect. 3 these limits assume Doppler imaging in only a single NIR band; observing slightly fainter objects should be feasible with broader wavelength coverage. Rhombus symbols indicate known directly-imaged giant exoplanets: a small number of these may be amenable to Doppler imaging with future large-aperture telescopes.

L9 object DENIS 0255-4700 (which has $\Delta F = 3\%$ and $v \sin i = 41.7 \pm 1.5$ km s^{-1}, but no measured period).

With ∼30 m-class telescopes, Fig. 4 demonstrates that Doppler imaging will become feasible for many dozens of substellar objects. Many of these will lie near the M/L transition, but at spectral types later than L5 at least 10–15 plausible candidates for these future studies already exist. As noted previously, measurements of photometric variability and $v \sin i$ are much less complete for later-type objects: thus many potential targets probably remain to be found.

Perhaps even more exciting, with these large new telescopes Doppler imaging of a small number of extrasolar giant planets may be possible. That this is plausible should not be too surprising, since HR 8799c has already been detected at good S/N using medium-resolution K band spectroscopy (Konopacky et al. 2013). The rhombus symbols in Fig. 4 indicate the magnitudes and approximate spectral types of several of the brightest known extrasolar planets (Chauvin et al. 2004, 2005; Marois et al. 2008, 2010; Lafrenière et al. 2008; Barman et al. 2011; Carson et al. 2013; Bonnefoy et al. 2013; Esposito et al. 2013). Of all these objects, the L2-type planet β Pic b seems the best candidate for Doppler imaging, with AB Pic b (L0) another possible target. These estimates are only approximate, since the spectral energy distributions of young, self-luminous planets differ from those of the brown dwarf spectra used in Sect. 3. Though variability and rotation parameters have not yet been reported for directly imaged planets, the analysis presented here suggests that such measurements – and eventually, Doppler imaging – might be feasible for these low-mass objects.

These estimated limits must of course be modulated by the level of photometric variability, which is not directly encapsulated by Fig. 4. As noted above, the sensitivity curves shown correspond to a photometric semi-amplitude of 3%, the median of the sample shown in Fig. 1b. Based on Eq. (1), for an object with variability f times this level the sensitivity curves in Fig. 4 should be shifted by $5 \log_{10} f$. Nonetheless, the trends described above will not change to the extent that variability amplitude and frequency are independent of spectral type (Buenzli et al. 2014).

4. Discussion, conclusions, and future work

I have presented the first quantitative investigation of the feasibility of Doppler imaging of brown dwarfs and extrasolar planets. The main results are summarized in Fig. 4, in terms of approximate limiting magnitudes for high-dispersion infrared spectrographs on 3.5 m, 8 m, and 30 m telescopes. K band offers the best prospects for Doppler imaging of objects with spectral types between L0 and T8, and sensitivity is also good at H band. Sensitivity is lower at J and L bands, but useful work should still be possible at these wavelengths for a smaller number of targets.

As part of this work I have also compiled all detections of photometric variability, rotation periods, and $v \sin i$ for substellar objects; these measurements are shown in Fig. 1 and listed in Table 2. Exceptionally bright and nearby brown dwarfs (such as

Luhman 16B), are feasible targets for Doppler imaging even on <4 m telescopes. With 8 m telescopes a few more objects can be observed, but the number of accessible objects with measured variability and/or rotation parameters are still small.

Doppler imaging of substellar objects will hit its stride with the next generation of giant ground-based telescopes, as shown in Fig. 4. Among objects already known, over 50 brown dwarfs with spectral types >M9 should be amenable to this analysis. In addition, Doppler imaging will likely be possible for a small number of young, self-luminous extrasolar giant planets.

The current sample of objects with measured variability, rotation, and/or $v \sin i$ is dominated by early-type objects and becomes quite sparse below ~L5 (see Fig. 1). However, T dwarfs occur more frequently in the Solar neighborhood than L dwarfs (Kirkpatrick et al. 2012); this suggests that many additional targets likely remain to be found. There is plenty of room at the bottom of the H-R diagram for new measurements of substellar rotation and variability and, eventually, for Doppler imaging.

Appendix: Data sources

Rotation periods

Individual references are listed in Table 2, and include the following: Artigau et al. (2009), Bailer-Jones & Mundt (2001), Berger et al. (2005, 2009), Biller et al. (2013), Buenzli et al. (2012), Caballero et al. (2004), Chew & Stassun (2009), Clarke et al. (2002b,a, 2008), Enoch et al. (2003), Gillon et al. (2013), Gizis et al. (2013), Hallinan et al. (2008), Harding et al. (2013b,a), Heinze et al. (2013), Irwin et al. (2011), Joergens et al. (2003), Khandrika et al. (2013), Koen (2003, 2005b, 2006, 2013b), Lane et al. (2007), Littlefair et al. (2006), Martín et al. (2006), Radigan et al. (2012, 2014), Rockenfeller et al. (2006a), Scholz et al. (2011), Wolszczan & Route (2014), and Zapatero Osorio et al. (2003, 2004).

Projected rotation velocity

Individual references for each object are listed in Table 2. Measurements were taken from the following references: Bailer-Jones (2004), Berger et al. (2008), Blake et al. (2007), Bochanski et al. (2011), Caballero et al. (2004), Crossfield et al. (2014), Del Burgo et al. (2009), Deshpande et al. (2012), Gizis et al. (2013), Joergens & Guenther (2001), Jones et al. (2005), Konopacky et al. (2012), Kurosawa et al. (2006), Martin et al. (1997), Mohanty et al. (2003, 2005), Muzerolle et al. (2003), Reid et al. (2002), Reiners & Basri (2006, 2008, 2010), Reiners et al. (2007), Rice et al. (2010), Snellen et al. (2014), Tinney & Reid (1998),White & Basri (2003), and Zapatero Osorio et al. (2004, 2006).

Variability

Individual references for measurements of significant photometric and/or spectroscopic variability, including the relevant bandpasses, are listed in Table 2. Data are taken from the following sources: Apai et al. (2013), Artigau et al. (2009), Bailer-Jones (2008), Bailer-Jones & Lamm (2003), Bailer-Jones & Mundt (1999, 2001), Berger et al. (2005, 2008, 2009), Bessell (1991), Biller et al. (2013), Buenzli et al. (2012, 2014), Burgasser et al. (2014), Carpenter et al. (2002), Chew & Stassun (2009), Clarke et al. (2002b,a, 2008), Cody & Hillenbrand (2010), Crossfield et al. (2014), Enoch et al. (2003), Gelino et al. (2002), Gillon et al. (2013), Girardin et al. (2013), Gizis et al. (2013), Goldman et al. (2008), Harding et al. (2013b,a), Heinze et al. (2013), Joergens et al. (2003), Irwin et al. (2011), Khandrika et al. (2013), Koen (2003, 2004, 2013b, 2005a, 2013a), Koen et al. (2004, 2005), Lane et al. (2007), Liebert et al. (2003), Littlefair et al. (2006, 2008), Maiti et al. (2005); Maiti (2007), Martín et al. (2001), Radigan et al. (2012, 2014), Reid et al. (2002), Reiners & Basri (2008), Rockenfeller et al. (2006b,a), Schmidt et al. (2007, 2014), Scholz & Eislöffel (2005); Scholz & Jayawardhana (2006); Scholz et al. (2011), Stelzer et al. (2006), Tinney & Tolley (1999), Wilson et al. (2014), and Zapatero Osorio et al. (2003, 2004). The interested reader might also consult the work of Rodríguez-Ledesma et al. (2009) to find a large number of variable candidates (>800) in the Orion Nebula Cluster (not included in this catalog).

Spectral type

Spectral types are the NIR classifications from the DwarfArchives.org website, from the literature, and from SIMBAD. Individual references are listed in Table 2. For completeness, the references used are: Allen et al. (2007), Artigau et al. (2006, 2010), Basri et al. (2000), Bonnefoy et al. (2013), Bouy et al. (2003), Burgasser et al. (2007); Burgasser & McElwain (2006); Burgasser et al. (2008, 2013), Burningham et al. (2010), Chiu et al. (2006), Close et al. (2003), Cruz et al. (2003, 2007, 2009), Cushing et al. (2011), Damjanov et al. (2007), Deacon et al. (2011), Fan et al. (2000), Forveille et al. (2005), Freed et al. (2003), Gizis (2002); Gizis et al. (2000a,b, 2001, 2011), Goto et al. (2002), Hawley et al. (2002), Hewett et al. (2006), Jenkins et al. (2009), Kendall et al. (2004, 2007), Kirkpatrick et al. (1995, 1999, 2000, 2008, 2010, 2011), Knapp et al. (2004), Kniazev et al. (2013), Kraus & Hillenbrand (2007), Leggett et al. (1994), Liebert et al. (2003), Lodieu et al. (2005), Luhman (2007), Martín et al. (1999, 2000), Mohanty et al. (2003, 2005), Phan-Bao et al. (2008), Potter et al. (2002), Reid et al. (2001, 2006, 2008), Reiners & Basri (2010), Rice et al. (2010), Salim et al. (2003), Schmidt et al. (2007, 2014), Seifahrt et al. (2010), Siegler et al. (2003, 2005), Stassun et al. (2007), Thorstensen & Kirkpatrick (2003), Tinney & Reid (1998); Tinney et al. (2005), Wilson et al. (2003), and Zapatero Osorio et al. (2006).

Binarity and separations

Reported binarity and measured separations are also included in the electronic version of Table 2. These are taken from SIMBAD and the work of Konopacky et al. (2010), Luhman (2013), Martín et al. (1999), McCaughrean et al. (2004), Probst (1983), Reid et al. (2000), Reid et al. (2001), Scholz (2010), White (1999), Wilson et al. (2014), and Zapatero Osorio et al. (2004)

Acknowledgements. I thank V. Jöergens for several excellent discussions that significantly improved the quality of the paper. I thank I. Snellen for interesting and stimulating discussions during the preparation of this work, and for his subsequent suggestions while acting as referee. This research has made use of the TOPCAT software package, and of free and open-source software provided by the Python, SciPy, and Matplotlib communities. This research has benefited from the M, L, T, and Y dwarf compendium housed at `DwarfArchives.org`, and from SIMBAD.

References

Allard, F. 2014, in IAU Symp. 299, eds. M. Booth, B. C. Matthews, & J. R. Graham, 271
Allen, P. R., Luhman, K. L., Myers, P. C., et al. 2007, ApJ, 655, 1095
Apai, D., Radigan, J., Buenzli, E., et al. 2013, ApJ, 768, 121

Artigau, É., Doyon, R., Lafrenière, D., et al. 2006, ApJ, 651, L57
Artigau, É., Bouchard, S., Doyon, R., & Lafrenière, D. 2009, ApJ, 701, 1534
Artigau, É., Radigan, J., Folkes, S., et al. 2010, ApJ, 718
Bailer-Jones, C. A. L. 2004, A&A, 419, 703
Bailer-Jones, C. A. L. 2008, MNRAS, 384, 1145
Bailer-Jones, C. A. L., & Lamm, M. 2003, MNRAS, 339, 477
Bailer-Jones, C. A. L., & Mundt, R. 1999, A&A, 348, 800
Bailer-Jones, C. A. L., & Mundt, R. 2001, A&A, 367, 218
Barman, T. S., Macintosh, B., Konopacky, Q. M., & Marois, C. 2011, ApJ, 733, 65
Basri, G., Mohanty, S., Allard, F., et al. 2000, ApJ, 538
Berger, E., Rutledge, R. E., Reid, I. N., et al. 2005, ApJ, 627, 960
Berger, E., Basri, G., Gizis, J. E., et al. 2008, ApJ, 676, 1307
Berger, E., Rutledge, R. E., Phan-Bao, N., et al. 2009, ApJ, 695, 310
Bessell, M. S. 1991, AJ, 101, 662
Biller, B. A., Crossfield, I. J. M., et al. 2013, ApJ, 778, L10
Blake, C. H., Charbonneau, D., White, R. J., Marley, M. S., & Saumon, D. 2007, ApJ, 666, 1198
Bochanski, J. J., Burgasser, A. J., Simcoe, R. A., & West, A. A. 2011, AJ, 142, 169
Bonnefoy, M., Boccaletti, A., Lagrange, A.-M., et al. 2013, A&A, 555, A107
Bouy, H., Brandner, W., Martín, E. L., et al. 2003, AJ, 126, 1526
Brandl, B. R., Lenzen, R., Pantin, E., et al. 2010, in SPIE Conf. Ser., 7735, 83
Brandl, B. R., Lenzen, R., Pantin, E., et al. 2012, in SPIE Conf. Ser., 8446
Brogi, M., Snellen, I. A. G., de Kok, R. J., et al. 2012, Nature, 486, 502
Buenzli, E., Apai, D., Morley, C. V., et al. 2012, ApJ, 760, L31
Buenzli, E., Apai, D., Radigan, J., Reid, I. N., & Flateau, D. 2014, ApJ, 782, 77
Burgasser, A. J., & McElwain, M. W. 2006, AJ, 131, 1007
Burgasser, A. J., Marley, M. S., Ackerman, A. S., et al. 2002, ApJ, 571, L151
Burgasser, A. J., Cruz, K. L., & Kirkpatrick, J. D. 2007, ApJ, 657, 494
Burgasser, A. J., Looper, D. L., Kirkpatrick, J. D., Cruz, K. L., & Swift, B. J. 2008, ApJ, 674, 451
Burgasser, A. J., Sheppard, S. S., & Luhman, K. L. 2013, ApJ, 772, 129
Burgasser, A. J., Gillon, M., Faherty, J. K., et al. 2014, ApJ, 785, 48
Burningham, B., Leggett, S. K., Lucas, P. W., et al. 2010, MNRAS, 404, 1952
Caballero, J. A., Béjar, V. J. S., Rebolo, R., & Zapatero Osorio, M. R. 2004, A&A, 424, 857
Caffau, E., Ludwig, H.-G., Steffen, M., Freytag, B., & Bonifacio, P. 2011, Sol. Phys., 268, 255
Carpenter, J. M., Hillenbrand, L. A., Skrutskie, M. F., & Meyer, M. R. 2002, AJ, 124, 1001
Carson, J., Thalmann, C., Janson, M., et al. 2013, ApJ, 763, L32
Chauvin, G., Lagrange, A.-M., Dumas, C., et al. 2004, A&A, 425, L29
Chauvin, G., Lagrange, A.-M., Zuckerman, B., et al. 2005, A&A, 438, L29
Chew, Y. G. M., & Stassun, K. G. 2009, in AIP Conf. Ser., 1119, eds. B. Karplus Hartline, R. K. Horton, & C. M. Kaicher, 208
Chiu, K., Fan, X., Leggett, S. K., et al. 2006, AJ, 131, 2722
Clarke, F. J., Oppenheimer, B. R., & Tinney, C. G. 2002a, MNRAS, 335, 1158
Clarke, F. J., Tinney, C. G., & Covey, K. R. 2002b, MNRAS, 332, 361
Clarke, F. J., Hodgkin, S. T., Oppenheimer, B. R., Robertson, J., & Haubois, X. 2008, MNRAS, 386, 2009
Close, L. M., Siegler, N., Freed, M., & Biller, B. 2003, ApJ, 587, 407
Cody, A. M., & Hillenbrand, L. A. 2010, ApJS, 191, 389
Collier Cameron, A. 1995, MNRAS, 275, 534
Cowan, N. B., & Agol, E. 2008, ApJ, 678, L129
Cowan, N. B., Fuentes, P. A., & Haggard, H. M. 2013, MNRAS, 434, 2465
Crepp, J. R., Bechter, A., Bechter, E., et al. 2014, in Am. Astron. Soc. Meet. Abst., 223, 34820
Crossfield, I. J. M., Barman, T., & Hansen, B. M. S. 2011, ApJ, 736, 132
Crossfield, I. J. M., Biller, B., Schlieder, J. E., et al. 2014, Nature, 505, 654
Cruz, K. L., Kirkpatrick, J. D., & Burgasser, A. J. 2009, AJ, 137, 3345
Cruz, K. L., Reid, I. N., Kirkpatrick, J. D., et al. 2007, AJ, 133, 439
Cruz, K. L., Reid, I. N., Liebert, J., Kirkpatrick, J. D., & Lowrance, P. J. 2003, AJ, 126, 2421
Cushing, M. C., Kirkpatrick, J. D., Gelino, C. R., et al. 2011, ApJ, 743, 50
Damjanov, I., Jayawardhana, R., Scholz, A., et al. 2007, ApJ, 670, 1337
Deacon, N. R., Liu, M. C., Magnier, E. A., et al. 2011, AJ, 142, 77
Del Burgo, C., Martín, E. L., Zapatero Osorio, M. R., & Hauschildt, P. H. 2009, A&A, 501, 1059
Deshpande, R., Martín, E. L., Montgomery, M. M., et al. 2012, AJ, 144, 99
Deutsch, A. J. 1958, in Electromagnetic Phenomena in Cosmical Physics, ed. B. Lehnert, IAU Symp., 6, 209
Donati, J., Semel, M., Carter, B. D., Rees, D. E., & Collier Cameron, A. 1997, MNRAS, 291, 658
Enoch, M. L., Brown, M. E., & Burgasser, A. J. 2003, AJ, 126, 1006
Esposito, S., Mesa, D., Skemer, A., et al. 2013, A&A, 549, A52
Fan, X., Knapp, G. R.,Strauss, M. A., et al. 2000, AJ, 119, 928
Forveille, T., Beuzit, J.-L., Delorme, P., et al. 2005, A&A, 435, L5
Freed, M., Close, L. M., & Siegler, N. 2003, ApJ, 584, 453
Freytag, B., Allard, F., Ludwig, H.-G., Homeier, D., & Steffen, M. 2011, in 16th Cambridge Workshop on Cool Stars, Stellar Systems, and the Sun, eds. C. Johns-Krull, M. K. Browning, & A. A. West, ASP Conf. Ser., 448, 855
Gelino, C. R., Marley, M. S., Holtzman, J. A., Ackerman, A. S., & Lodders, K. 2002, ApJ, 577, 433
Gillon, M., Triaud, A. H. M. J., Jehin, E., et al. 2013, A&A, 555, L5
Gilmozzi, R., & Spyromilio, J. 2007, The Messenger, 127, 11
Girardin, F., Artigau, É., & Doyon, R. 2013, ApJ, 767, 61
Gizis, J. E. 2002, ApJ, 575, 484
Gizis, J. E., Monet, D. G., Reid, I. N., Kirkpatrick, J. D., & Burgasser, A. J. 2000a, MNRAS, 311, 385
Gizis, J. E., Monet, D. G., Reid, I. N., et al. 2000b, AJ, 120, 1085
Gizis, J. E., Kirkpatrick, J. D., & Wilson, J. C. 2001, AJ, 121, 2185
Gizis, J. E., Troup, N. W., & Burgasser, A. J. 2011, ApJ, 736, L34
Gizis, J. E., Burgasser, A. J., Berger, E., et al. 2013, ApJ, 779, 172
Goldman, B., Cushing, M. C., Marley, M., et al. 2008, A&A, 487, 277
Golimowski, D. A., Leggett, S. K., Marley, M. S., et al. 2004, AJ, 127, 3516
Goto, M., Kobayashi, N., Terada, H., et al. 2002, ApJ, 567, L59
Greene, T. P., Tokunaga, A. T., Toomey, D. W., & Carr, J. B. 1993, in Infrared Detectors and Instrumentation, ed. A. M. Fowler, SPIE Conf. Ser., 1946, 313
Hallinan, G., Antonova, A., Doyle, J. G., et al. 2008, ApJ, 684, 644
Harding, L. K., Hallinan, G., Boyle, R. P., et al. 2013a, ApJ, 779, 101
Harding, L. K., Hallinan, G., Konopacky, Q. M., et al. 2013b, A&A, 554, A113
Hatzes, A. P. 1998, A&A, 330, 541
Hawley, S. L., Covey, K. R., Knapp, G. R., et al. 2002, AJ, 123, 3409
Heinze, A. N., Metchev, S., Apai, D., et al. 2013, ApJ, 767, 173
Hewett, P. C., Warren, S. J., Leggett, S. K., & Hodgkin, S. T. 2006, MNRAS, 367, 454
Hinkle, K. H., Cuberly, R. W., Gaughan, N. A., et al. 1998, in Infrared Astronomical Instrumentation, ed. A. M. Fowler, SPIE Conf. Ser., 3354, 810
Hinkle, K. H., Wallace, L., & Livingston, W. 2003, BAAS, 35, 1260
Irwin, J., Berta, Z. K., Burke, C. J., et al. 2011, ApJ, 727, 56
Jaffe, D. T., Mar, D. J., Warren, D., & Segura, P. R. 2006, in SPIE Conf. Ser., 6269
Jardine, M., Barnes, J. R., Donati, J.-F., & Collier Cameron, A. 1999, MNRAS, 305, L35
Jenkins, J. S., Ramsey, L. W., Jones, H. R. A., et al. 2009, ApJ, 704, 975
Joergens, V., & Guenther, E. 2001, A&A, 379, L9
Joergens, V., Fernández, M., Carpenter, J. M., & Neuhäuser, R. 2003, ApJ, 594, 971
Johns, M. 2008, in SPIE Conf. Ser., 6986
Jones, H. R. A., Pavlenko, Y., Viti, S., et al. 2005, MNRAS, 358, 105
Kaeufl, H.-U. et al. 2004, in SPIE Conf. Ser. 5492, eds. A. F. M. Moorwood, & M. Iye, 1218
Kendall, T. R., Delfosse, X., Martín, E. L., & Forveille, T. 2004, A&A, 416, L17
Kendall, T. R., Jones, H. R. A., Pinfield, D. J., et al. 2007, MNRAS, 374, 445
Khandrika, H., Burgasser, A. J., Melis, C., et al. 2013, AJ, 145, 71
Kirkpatrick, J. D., Henry, T. J., & Simons, D. A. 1995, AJ, 109, 797
Kirkpatrick, J. D., Reid, I. N., Liebert, J., et al. 1999, ApJ, 519, 802
Kirkpatrick, J. D., Reid, I. N., Liebert, J., et al. 2000, AJ, 120, 447
Kirkpatrick, J. D., Cruz, K. L., Barman, T. S., et al. 2008, ApJ, 689, 1295
Kirkpatrick, J. D., Looper, D. L., Burgasser, A. J., et al. 2010, ApJS, 190, 100
Kirkpatrick, J. D., Cushing, M. C., Gelino, C. R., et al. 2011, ApJS, 197, 19
Kirkpatrick, J. D., Gelino, C. R., Cushing, M. C., et al. 2012, ApJ, 753, 156
Knapp, G. R., Leggett, S. K., Fan, X., et al. 2004, AJ, 127, 3553
Kniazev, A. Y., Vaisanen, P., Mužić, K., et al. 2013, ApJ, 770, 124
Knutson, H. A., Lewis, N., Fortney, J. J., et al. 2012, ApJ, 754, 22
Koen, C. 2003, MNRAS, 346, 473
Koen, C. 2004, MNRAS, 354, 378
Koen, C. 2005a, MNRAS, 360, 1132
Koen, C. 2005b, MNRAS, 357, 1151
Koen, C. 2006, MNRAS, 367, 1735
Koen, C. 2013a, MNRAS, 428, 2824
Koen, C. 2013b, MNRAS, 429, 652
Koen, C., Matsunaga, N., & Menzies, J. 2004, MNRAS, 354, 466,
Koen, C., Tanabé, T., Tamura, M., & Kusakabe, N. 2005, MNRAS, 362, 727
Konopacky, Q. M., Ghez, A. M., Barman, T. S., et al. 2010, ApJ, 711, 1087
Konopacky, Q. M., Ghez, A. M., Fabrycky, D. C., et al. 2012, ApJ, 750, 79
Konopacky, Q. M., Barman, T. S., Macintosh, B. A., & Marois, C. 2013, Science, 339, 1398
Kraus, A. L., & Hillenbrand, L. A. 2007, AJ, 134, 2340
Kurosawa, R., Harries, T. J., & Littlefair, S. P. 2006, MNRAS, 372, 1879
Lafrenière, D., Jayawardhana, R., & van Kerkwijk, M. H. 2008, ApJ, 689, L153
Lane, C., Hallinan, G., Zavala, R. T., et al. 2007, ApJ, 668, L163
Lee, S., Yuk, I.-S., Lee, H., et al. 2010, in SPIE Conf. Ser., 7735
Leggett, S. K., Harris, H. C., & Dahn, C. C. 1994, AJ, 108, 944
Liebert, J., Kirkpatrick, J. D., Cruz, K. L., et al. 2003, AJ, 125, 343

Littlefair, S. P., Dhillon, V. S., Marsh, T. R., Shahbaz, T., & Martín, E. L. 2006, MNRAS, 370, 1208
Littlefair, S. P., Dhillon, V. S., Marsh, T. R., et al. 2008, MNRAS, 391, L88
Lodieu, N., Scholz, R.-D., McCaughrean, M. J., et al. 2005, A&A, 440, 1061
Looper, D. L., Gelino, C. R., Burgasser, A. J., & Kirkpatrick, J. D. 2008, ApJ, 685, 1183
Lord, S. D. 1992, A new software tool for computing Earth's atmospheric transmission of near- and far-infrared radiation, Tech. Rep.
Luhman, K. L. 2007, ApJS, 173, 104
Luhman, K. L. 2013, ApJ, 767, L1
Mahadevan, S., Ramsey, L., Bender, C., et al. 2012, in SPIE Conf. Ser., 8446
Maiolino, R., Haehnelt, M., Murphy, M. T., et al. 2013 [arXiv:1310.3163]
Maiti, M. 2007, AJ, 133, 1633
Maiti, M., Sengupta, S., Parihar, P. S., & Anupama, G. C. 2005, ApJ, 619, L183
Marois, C., Macintosh, B., Barman, T., et al. 2008, Science, 322, 1348
Marois, C., Zuckerman, B., Konopacky, Q. M., Macintosh, B., & Barman, T. 2010, Nature, 468, 1080
Martin, E. L., Basri, G., Delfosse, X., & Forveille, T. 1997, A&A, 327, L29
Martín, E. L., Delfosse, X., Basri, G., et al. 1999, AJ, 118, 2466
Martín, E. L., Brandner, W., Bouvier, J., et al. 2000, ApJ, 543, 299
Martín, E. L., Dougados, C., Magnier, E., et al. 2001, ApJ, 561, L195
Martín, E. L., Guenther, E., Zapatero Osorio, M. R., Bouy, H., & Wainscoat, R. 2006, ApJ, 644, L75
McCarthy, D. W., Burge, J. H., Angel, J. R. P., et al. 1998, in Infrared Astronomical Instrumentation, ed. A. M. Fowler, SPIE Conf. Ser., 3354, 750
McCaughrean, M. J., Close, L. M., Scholz, R.-D., et al. 2004, A&A, 413, 1029
McLean, I. S., Becklin, E. E., Bendiksen, O., et al. 1998, in SPIE Conf. Ser., 3354, ed. A. M. Fowler, 566
Mohanty, S., Jayawardhana, R., & Barrado y Navascués, D. 2003, ApJ, 593, L109
Mohanty, S., Jayawardhana, R., & Basri, G. 2005, ApJ, 626, 498
Muzerolle, J., Hillenbrand, L., Calvet, N., Briceño, C., & Hartmann, L. 2003, ApJ, 592, 266
Nelson, J., & Sanders, G. H. 2008, in SPIE Conf. Ser., 7012
Oliva, E., Origlia, L., Maiolino, R., et al. 2012, in SPIE Conf. Ser., 8446
Phan-Bao, N., Bessell, M. S., Martín, E. L., et al. 2008, MNRAS, 383, 831
Piskunov, N. E., & Rice, J. B. 1993, PASP, 105, 1415
Potter, D., Martín, E. L., Cushing, M. C., et al. 2002, ApJ, 567, L133
Probst, R. G. 1983, ApJS, 53, 335
Quirrenbach, A., Amado, P. J., Seifert, W., et al. 2012, in SPIE Conf. Ser., 8446
Radigan, J., Jayawardhana, R., Lafrenière, D., et al. 2012, ApJ, 750, 105
Radigan, J., Lafrenière, D., Jayawardhana, R., & Artigau, E. 2014, ApJ, accepted [arXiv:1404.3247]
Rayner, J., Bond, T., Bonnet, M., Jaffe, D., Muller, G., & Tokunaga, A. 2012, in SPIE Conf. Ser., 8446
Reid, I. N., Kirkpatrick, J. D., Gizis, J. E., et al. 2000, AJ, 119, 369
Reid, I. N., Gizis, J. E., Kirkpatrick, J. D., & Koerner, D. W. 2001, AJ, 121, 489
Reid, I. N., Kirkpatrick, J. D., Liebert, J., et al. 2002, AJ, 124, 519
Reid, I. N., Lewitus, E., Allen, P. R., Cruz, K. L., & Burgasser, A. J. 2006, AJ, 132, 891
Reid, I. N., Cruz, K. L., Kirkpatrick, J. D., et al. 2008, AJ, 136, 1290
Reiners, A., & Basri, G. 2006, AJ, 131, 1806
Reiners, A., & Basri, G. 2008, ApJ, 684, 1390
Reiners, A., & Basri, G. 2010, ApJ, 710, 924
Reiners, A., Seifahrt, A., Stassun, K. G., Melo, C., & Mathieu, R. D. 2007, ApJ, 671, L149
Rice, J. B. 2002, Astron. Nachr., 323, 220
Rice, E. L., Barman, T., Mclean, I. S., Prato, L., & Kirkpatrick, J. D. 2010, ApJS, 186, 63
Rockenfeller, B., Bailer-Jones, C. A. L., & Mundt, R. 2006a, A&A, 448, 1111
Rockenfeller, B., Bailer-Jones, C. A. L., Mundt, R., & Ibrahimov, M. A. 2006b, MNRAS, 367, 407
Rodler, F., Lopez-Morales, M., & Ribas, I. 2012, ApJ, 753, L25
Rodríguez-Ledesma, M. V., Mundt, R., & Eislöffel, J. 2009, A&A, 502, 883
Salim, S., Lépine, S., Rich, R. M., & Shara, M. M. 2003, ApJ, 586, L149
Schmidt, S. J., Cruz, K. L., Bongiorno, B. J., Liebert, J., & Reid, I. N. 2007, AJ, 133, 2258
Schmidt, S. J., Prieto, J. L., Stanek, K. Z., et al. 2014, ApJ, 781, L24
Scholz, A., & Eislöffel, J. 2005, A&A, 429, 1007
Scholz, A., & Jayawardhana, R. 2006, ApJ, 638, 1056
Scholz, R.-D. 2010, A&A, 510, L8
Scholz, R.-D., Bihain, G., Schnurr, O., & Storm, J. 2011, A&A, 532, L5
Seifahrt, A., Reiners, A., Almaghrbi, K. A. M., & Basri, G. 2010, A&A, 512, A37
Showman, A. P., & Kaspi, Y. 2013, ApJ, 776, 85
Siegler, N., Close, L. M., Mamajek, E. E., & Freed, M. 2003, ApJ, 598, 1265
Siegler, N., Close, L. M., Cruz, K. L., Martín, E. L., & Reid, I. N. 2005, ApJ, 621, 1023
Skrutskie, M. F. et al. 2006, AJ, 131, 1163
Snellen, I. A. G., de Kok, R. J., de Mooij, E. J. W., & Albrecht, S. 2010, Nature, 465, 1049
Snellen, I., Brandl, B., de Kok, R., Brogi, M., Birkby, J., & Schwarz, H. 2014, Nature, in press
Stassun, K. G., Mathieu, R. D., & Valenti, J. A. 2007, ApJ, 664, 1154
Stelzer, B., Schmitt, J. H. M. M., Micela, G., & Liefke, C. 2006, A&A, 460, L35
Stephens, D. C., Leggett, S. K., Cushing, M. C., et al. 2009, ApJ, 702, 154
Strassmeier, K. G. 2009, A&ARv, 17, 251
Tamura, M., Suto, H., Nishikawa, J., et al. 2012, in SPIE Conf. Ser., 8446, 84461T
Thibault, S., Rabou, P., Donati, J.-F., et al. 2012, in SPIE Conf. Ser., 8446, 30
Thorstensen, J. R., & Kirkpatrick, J. D. 2003, PASP, 115, 1207
Tinney, C. G., & Reid, I. N. 1998, MNRAS, 301, 1031
Tinney, C. G., & Tolley, A. J. 1999, MNRAS, 304, 119
Tinney, C. G., Burgasser, A. J., Kirkpatrick, J. D., & McElwain, M. W. 2005, AJ, 130, 2326
TMT Project 2013, TMT Science-based Requirements Document, TMT document number TMT.PSC.DRD.05.001.CCR19, Tech. Rep.
Tokunaga, A. T., Kobayashi, N., Bell, J., et al. 1998, in Infrared Astronomical Instrumentation, ed. A. M. Fowler, SPIE Conf. Ser., 3354, 512
Vogt, S. S. 1987, in Liège International Astrophysical Colloq., 27, eds. J.-P. Swings, J. Collin, & E. J. Wampler, 317
White, R. J. 1999, Ph.D. Thesis, University of Texas at Austin, USA
White, R. J., & Basri, G. 2003, ApJ, 582, 1109
Wilson, J. C., Miller, N. A., Gizis, J. E., et al. 2003, in Brown Dwarfs, ed. E. Martín, IAU Symp., 211, 197
Wilson, P. A., Rajan, A., & Patience, J. 2014, A&A, in press, DOI: 10.1051/0004-6361/201322995
Wolszczan, A., & Route, M. 2014, ApJ, accepted
Yuk, I.-S., Jaffe, D. T., Barnes, S., et al. 2010, in SPIE Conf. Ser., 7735, 54
Zapatero Osorio, M. R., Caballero, J. A., Béjar, V. J. S., & Rebolo, R. 2003, A&A, 408, 663
Zapatero Osorio, M. R., Lane, B. F., Pavlenko, Y., et al. 2004, ApJ, 615, 958
Zapatero Osorio, M. R., Martín, E. L., Bouy, H., et al. 2006, ApJ, 647, 1405
Zhang, X., & Showman, A. P. 2014, ApJ, 788, 6